

S-Allylcysteine inhibits tumour progression and the epithelial–mesenchymal transition in a mouse xenograft model of oral cancer

Man-Hui Pai¹, Yueh-Hsiung Kuo², En-Pei Isabel Chiang³ and Feng-Yao Tang^{4*}

¹Department of Anatomy, Taipei Medical University, 11031 Taipei, Taiwan, ROC

²Tsuzuki Institute for Traditional Medicine, Graduate Institute of Pharmaceutical Chemistry, China Medical University, Taichung 40402, Taiwan, ROC

³Department of Food Science and Biotechnology, National Chung-Hsing University, Taichung 402, Taiwan, ROC

⁴Biomedical Science Laboratory, Department of Nutrition, China Medical University, 91 Hsueh-Shih Road, 40402 Taichung, Taiwan, ROC

(Submitted 14 January 2011 – Final revision received 17 August 2011 – Accepted 17 August 2011 – First published online 20 October 2011)

Abstract

Oral cancer is prevalent worldwide. Studies have indicated that an increase in the osteopontin (OPN) plasma level is correlated with the progression of oral cancer. Our previous report showed that the aqueous garlic extract *S*-allylcysteine (SAC) inhibited the epithelial–mesenchymal transition (EMT) of human oral cancer CAL-27 cells *in vitro*. Therefore, the present study investigated whether SAC consumption would help prevent tumour growth and progression, including the EMT, in a mouse xenograft model of oral cancer. The results demonstrated that SAC dose-dependently inhibited the growth of oral cancer in tumour-bearing mice. The histopathological and immunohistochemical staining results indicated that SAC was able to effectively suppress the tumour growth and progression of oral cancer *in vivo*. The chemopreventive effect of SAC was associated with the suppression of carcinogenesis factors such as *N*-methylpurine DNA glycosylase and OPN. SAC significantly suppressed the phosphorylation of Akt, mammalian target of rapamycin, inhibitor of κ B α and extracellular signal-regulated kinase 1/2 in tumour tissues. The results demonstrated that the SAC-mediated suppression of cyclin D1 protein was associated with an augmented expression of the cell-cycle inhibitor p16^{Ink4}. Furthermore, SAC inhibited the expression of cyclo-oxygenase-2, vimentin and NF- κ B p65 (RelA). These results show that SAC has potential as an agent against tumour growth and the progression of oral cancer in a mouse xenograft model.

Key words: *S*-Allylcysteine; Osteopontin; Vimentin; Cyclo-oxygenase-2; Human oral cancer cells

Oral cancer is one of the most prevalent types of cancer in the world today⁽¹⁾. It is well known that oral cancer is characterised by the aberrant proliferation and invasion of malignant cells into the underlying connective tissues⁽¹⁾. Recent studies have suggested a strong correlation between the osteopontin (OPN) plasma level and oral carcinogenesis⁽²⁾. OPN activates a number of different signalling pathways, thus exerting an effect on the migration, proliferation and survival of cancer cells^(3,4). For example, the phosphatidylinositol-3-kinase (PI3K)/Akt/mammalian target of rapamycin (mTOR) and mitogen-activated protein kinase (MAPK)/extracellular signal-regulated

kinase (ERK) signalling cascades play important roles in tumour growth and progression^(5–7).

The Akt/mTOR proteins regulate cell-cycle progression, growth-factor-mediated survival and tumour cell growth^(8,9). Upon the activation of the PI3K signalling pathway, the NF- κ B inhibitor protein (inhibitor of κ B; I κ B) is phosphorylated by I κ B α kinase and then subjected to ubiquitin-mediated degradation⁽¹⁰⁾. The degradation of I κ B permits the translocation of activated NF- κ B from the cytoplasm into the nucleus, where it up-regulates cyclo-oxygenase-2 (COX-2) gene expression and thus triggers the progression of oral cancer⁽¹¹⁾. COX-2 protein is responsible for the production

Abbreviations: AGE, aged garlic extract; BW, body weight; COX-2, cyclo-oxygenase-2; DMEM, Dulbecco's modified Eagle's medium; EMT, epithelial–mesenchymal transition; ERK, extracellular signal-regulated kinase; I κ B, inhibitor of κ B; MAPK, mitogen-activated protein kinase; MPG, *N*-methylpurine DNA glycosylase; mTOR, mammalian target of rapamycin; OPN, osteopontin; PCNA, proliferating cell nuclear antigen; PI3K, phosphatidylinositol-3-kinase; SAC, *S*-allylcysteine.

* **Corresponding author:** Dr F.-Y. Tang, fax +886 4 22062891, email vincenttang@mail.cmu.edu.tw

of PG and tumour-associated inflammation⁽¹²⁾. Several studies have reported that the expression of NF- κ B and COX-2 proteins is associated with treatment resistance in oral cancer⁽¹³⁾.

Overactivated MAPK/ERK signalling pathways have been reported to be involved in accelerated cell-cycle progression and the proliferation of cancer cells⁽¹⁴⁾. During the proliferation of oral cancer cells, cell-cycle-related proteins, such as cyclin D1 and proliferating cell nuclear antigen (PCNA), function as major regulators of cell-cycle progression and DNA replication, respectively⁽¹⁵⁾. Recent studies have indicated that p16^{Ink4} protein may serve as a cell-cycle inhibitor and suppress the activity of cyclin D1 and PCNA proteins^(16,17). Taken together, the PI3K/Akt/mTOR, MAPK/ERK and NF- κ B signalling pathways play crucial roles in both OPN-mediated tumour growth and the poor prognosis associated with oral cancer.

A recent study has also indicated that COX-2 expression is associated with the epithelial–mesenchymal transition (EMT) in various types of human cancer^(18,19). Many studies have indicated that the EMT is a critical cellular mechanism, which plays an important role in tumour progression and metastasis in many types of cancer, including oral cancer^(20,21). E-cadherin complexes are major constituents of the epithelial junctions in the normal oral epithelium⁽²²⁾. The loss of E-cadherin and the augmented expression of vimentin are considered to be key steps in the EMT and tumour progression^(21,23). However, suppression of the ERK1/2 and PI3K/Akt/NF- κ B signalling cascades induces the mesenchymal-to-epithelial reverting transition along with increasing E-cadherin expression in cancer cells^(21,24). Therefore, these results suggest that the MAPK/ERK and PI3K/Akt/NF- κ B signalling pathways and COX-2 are associated with the EMT process in human oral cancer. Clinical studies have indicated that increases in OPN plasma levels over time are significantly associated with poor patient survival⁽²⁵⁾. Therefore, any therapeutic application or nutritional intervention that resulted in a suppression of COX-2 or OPN proteins might be an effective approach to the treatment of oral cancer^(26–28).

Studies have shown that *N*-methylpurine DNA glycosylase (MPG), a DNA repair enzyme that repairs *N*-alkylpurine damage, is up-regulated in cancer cell lines⁽²⁹⁾. Overexpression of this enzyme contributes to chromatid exchange, chromosomal aberration and genetic mutation, possibly due to incomplete excision repair⁽³⁰⁾. Therefore, MPG is considered a promoter of carcinogenesis⁽²⁹⁾. In the course of considering the role of DNA lesions in mutagenesis and carcinogenesis, we also investigated MPG expression.

Epidemiological studies have suggested that the consumption of garlic extracts exerts a protective effect against various types of cancer, including prostate, colon and oral cancers^(31,32). Garlic contains certain lipid-soluble and water-soluble anticancer constituents⁽³³⁾. The lipid-soluble garlic constituents include diallyl sulphide, diallyl disulphide and diallyl trisulphide. The water-soluble garlic constituents include *S*-allylcysteine (SAC) and *S*-allylmercaptocysteine. SAC is abundant in aged garlic extract (AGE). AGE is produced by the immersion and extraction of raw garlic in aqueous ethanol for more than 10 months at room temperature.

During the process, most of the orangesulphur compounds are changed naturally into more stable and bioavailable water-soluble compounds. Studies have shown that the active ingredients in garlic (*Allium sativum*) extracts, including diallyl disulphide and diallyl trisulphide, effectively inhibit the proliferation of cancer cells^(34–38). It has also been reported that SAC suppresses the growth of several types of cancer^(39–41). Our previous study has shown that SAC inhibited the proliferation of human oral cancer CAL-27 cells *in vitro*⁽⁴²⁾. Moreover, it has been reported that SAC prevents the EMT and suppresses tumour progression in human oral squamous cancer cells *in vitro*⁽⁴²⁾. However, the *in vivo* inhibitory effects of SAC on tumour growth and progression in oral cancer have not been demonstrated. The present study was undertaken to evaluate the *in vivo* anticancer effects of SAC, including the inhibition of tumour growth and progression. Immunodeficient nude mice with xenografted human oral cancer CAL-27 cells under the skin comprised the experimental model. It was demonstrated that the consumption of SAC significantly inhibited both tumour growth and the progression of oral cancer in this mouse xenograft model.

Materials and methods

Reagents and antibodies

SAC was purchased from LKT laboratories, Inc. (St Paul, MN, USA). Anti-phospho-Akt, anti-phospho-mTOR, anti-phospho-I κ B α , anti-phospho-ERK 1/2, anti-E-cadherin, anti-p16^{Ink4}, anti-cyclin D1, anti-NF- κ B p65 (RelA), anti-vimentin and anti-COX-2 monoclonal antibodies were purchased from Cell Signaling Technology, Inc. (Danvers, MA, USA). Anti- β -actin antibody was purchased from Sigma (St Louis, MO, USA). Anti-MPG and anti-PCNA antibodies were purchased from Santa Cruz Biotechnology (Santa Cruz, CA, USA). The human oral cancer CAL-27 cell line was obtained from the American Type Culture Collection (Manassas, VA, USA). Dulbecco's modified Eagle's medium (DMEM)/F12 medium was purchased from Invitrogen Inc. (Carlsbad, CA, USA). Tissue nuclear extraction reagent and tissue lysis kits were purchased from Pierce Biotechnology Inc. (Rockford, IL, USA). PBS, fluorescein isothiocyanate and rhodamine were purchased from Invitrogen Inc. The OPN ELISA kit was purchased from R&D Systems, Inc. (Minneapolis, MN, USA). SAC was dissolved in distilled water at a concentration of 400 mM and stored at -20°C . Immediately before the experiment, various concentrations of the SAC solution were freshly prepared and given to the experimental animals.

Cell culture

Human oral cancer CAL-27 cells were cultured in a 37°C humidified incubator with 5% CO₂ and grown to confluency using fetal bovine serum-supplemented DMEM/F12 media. The DMEM/F12 medium was supplemented with 10% heat-inactivated fetal bovine serum, 2 mM-L-glutamine and 1.5 g sodium bicarbonate/l in the absence of antibiotics.

Xenograft implantation of tumour cells

Human oral cancer CAL-27 cells were maintained at 37°C in a 5% CO₂ incubator and grown to confluency using DMEM/F12 media supplemented with 10% fetal bovine serum and 0.15% (w/v) sodium bicarbonate. To establish the mouse xenograft model, subconfluent cultures of oral cancer CAL-27 cells were given fresh medium 24 h before being harvested by a brief treatment with 0.25% trypsin and 0.02% EDTA. Trypsinisation was stopped with medium containing 10% fetal bovine serum, and the cells were washed twice and resuspended in serum-free medium. Only single-cell suspensions with a viability of >90% were used for the injections.

Animals, diet and S-allylcysteine supplementation

Adult (3–4 weeks old) BALB/C AnN-Foxn1 nude mice (22–25 g) were obtained from the National Laboratory Animal Center (Taipei, Taiwan). Mice were maintained under specific pathogen-free conditions in facilities approved by the National Laboratory Animal Center in accordance with current regulations and standards (animal protocol no. 97-5-D). During the entire experimental period, mice were fed a standard Lab 5010 diet purchased from LabDiet Inc. (St Louis, MO, USA). The standard diet contained crude fat (13.5% total diet energy), protein (27.5% total diet energy) and carbohydrate (59% total diet energy), and had no detectable amounts of SAC, as indicated by the supplier.

Mice that had been anaesthetised with inhaled isoflurane were placed in a supine position. Then each BALB/C AnN-Foxn1 nude mouse was subcutaneously injected with approximately one million human oral cancer CAL-27 cells into the right flank. A well-localised bleb was considered to be a sign of a technically satisfactory injection. After the inoculation, mice were divided into three subgroups. SAC was dissolved in distilled water and given to the experimental animals by oral administration once per d at a total volume of 0.15 ml. One group (low-dose SAC) received a daily oral consumption dose of SAC dissolved in distilled water at 5 mg/kg body weight (BW) once per d. The other group (high-dose SAC) received SAC at an oral dose of 40 mg/kg BW once per d. The tumour control group did not receive any SAC supplementation. To measure OPN plasma levels, tumour-free mice were used as the normal control group. Both the normal control group and the tumour control group received only distilled water instead of treatment. Tumour volume was calculated by the following formula: $0.524 L_1(L_2)^2$, where L_1 and L_2 represent the long and short axis of the tumour, respectively. BW was determined once weekly. At the end of the experimental period, animals were euthanised with CO₂ inhalation; tumour tissues were then excised, weighed and frozen for further experiments.

The remaining tissues of liver, lung, spleen, pancreas and intestine were also frozen immediately, sectioned and stained with Mayer's haematoxylin–eosin for light microscopy. Blood samples were collected from the heart into a 1 ml vacutainer tube containing heparin and centrifuged for 10 min at 1000 g to obtain plasma.

Histopathological, immunohistochemical and immunofluorescent staining of tumour tissues

Frozen tumour tissues were cut in 5 µm sections and immediately fixed with 4% paraformaldehyde. Sections were stained with Mayer's haematoxylin–eosin for light microscopy. Negative controls did not exhibit any staining. In a blinded manner, three hot spots were examined per tumour section (high-power fields 400 ×) of six different tumours in each group. Images of tumour sections were acquired on an Olympus BX-51 microscope using an Olympus DP-71 digital camera and imaging system (Olympus, Tokyo, Japan).

For immunohistochemical staining, frozen tissue sections were treated with 0.3% H₂O₂ to block the endogenous peroxidase activity. Non-specific protein bindings were blocked with 10% normal goat serum for 1 h followed by incubation with an anti-MPG primary antibody (1:300). Tissue sections were washed with 0.1 M-PBS and incubated with biotinylated immunoglobulin G (1:300 secondary antibody) at room temperature for 1 h. Tissue sections were stained with avidin–biotin complex, diaminobenzidine and H₂O₂. Cell nuclei were stained with haematoxylin. Imaging was performed at 200 × and 400 × magnification. Images of tumour sections were acquired on an Olympus BX-51 microscope using an Olympus DP-71 digital camera and imaging system.

For immunofluorescent staining, primary oral cancer tissues were frozen, sectioned and subjected to anti-PCNA, anti-vimentin and anti-COX-2 antibodies. The sectioned tissues that were probed with anti-PCNA antibody or anti-vimentin antibody were further subjected to a secondary antibody with an anti-IgG-conjugated fluorescein isothiocyanate label. The sectioned tissues that were probed with anti-COX-2 antibody were further subjected to a secondary antibody with a rhodamine label. Cell nuclei were stained with 4,6-diamidino-2-phenyl indole. Imaging was performed at 400 × magnification. Images of the tumour sections were acquired on an Olympus BX-51 microscope using an Olympus DP-71 digital camera and imaging system.

Protein extraction

Briefly, animal tissues were prepared using a Tissue Nuclear Extract Reagent Kit (Pierce Biotechnology Inc., Rockford, IL, USA) containing protease and phosphatase inhibitors, according to the manufacturer's instructions. After centrifugation for 10 min at 12 000 g to remove cell debris, the supernatants were further separated and retained as cytoplasmic and nuclear fraction extracts, respectively. Cross-contamination between the nuclear and cytoplasmic fractions was not found (data not shown).

Western blotting analysis

The cytoplasmic and nuclear fractions of tissue proteins (60 µg) were fractionated on 10% SDS-PAGE, transferred to a nitrocellulose membrane and blotted with an anti-phosphorylation Akt monoclonal antibody, according to the manufacturer's instructions. The blots were stripped

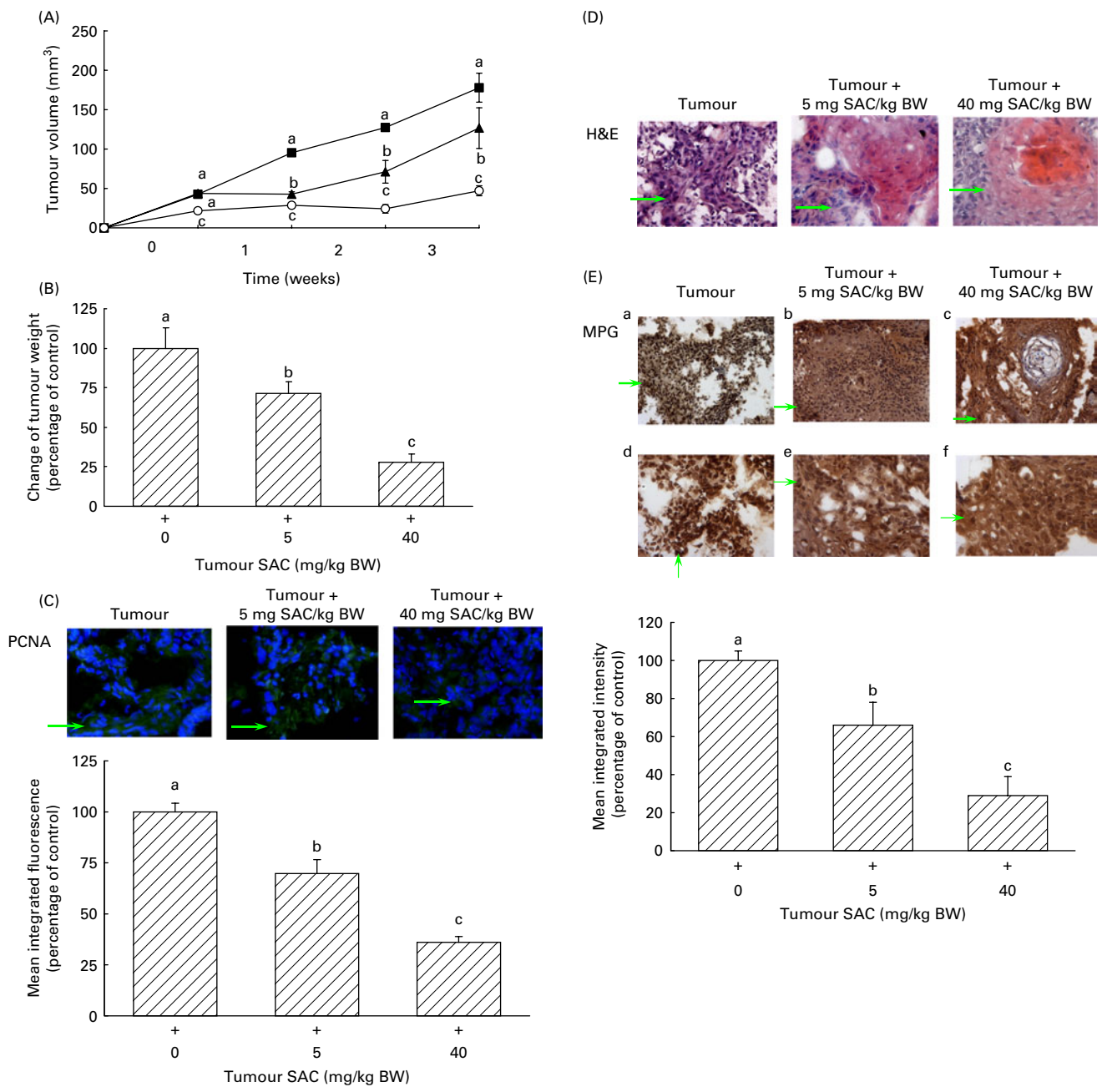


Fig. 1. S-allylcysteine (SAC) inhibited tumour growth and the progression of oral cancer in a mouse xenograft model. (A) Xenograft nude mice (n 6 per group) were divided into three groups (tumour, tumour with low SAC, tumour with high SAC) and given SAC (0, 5 and 40 mg/kg body weight (BW) per d) for 4 weeks. The extent of tumour growth was evaluated by the measurement of the tumour volume. The data on the tumour volume represent the proliferation index in primary tumour tissues. ^{a,b,c}Values with unlike letters are significantly different at each time point ($P < 0.05$). —■—, Tumour; —▲—, tumour + 5 mg SAC/kg BW; —○—, tumour + 40 mg SAC/kg BW. (B) Data represent the change in tumour weight among the control, low_SAC (5 mg/kg BW per d) and high_SAC (40 mg/kg BW per d) groups. ^{a,b,c}Values with unlike letters are significantly different at week 4 ($P < 0.05$). (C) Samples from the different groups of oral cancer tissue were frozen, sectioned and subjected to anti-proliferating cell nuclear antigen (PCNA) antibody by immunofluorescent staining described in the Materials and methods section. Imaging was documented at 400 × magnification. The green fluorescence area represented the distribution of the PCNA protein in CAL-27 cells stained with a monoclonal antibody. The blue fluorescence area represented the location of cell nuclei stained with 4,6-diamidino-2-phenyl indole. The mean integrated fluorescence of the PCNA protein is shown in the bottom panel. ^{a,b,c}Values with unlike letters are significantly different ($P < 0.05$). (D) The oral cancer tissues were formalin-fixed, embedded in paraffin, sectioned and subjected to haematoxylin–eosin (H&E) staining. Imaging was documented at 400 × magnification. The blue spots indicated with the green arrows represent the nuclei stained with haematoxylin. The red spots are the cytoplasm stained with eosin. (E) The oral cancer tissues were frozen, sectioned and subjected to anti-*N*-methylpurine DNA glycosylase (MPG) antibody by immunohistochemical staining described in the Materials and methods section. Imaging was performed at 200 × (a–c) and 400 × (d–f) magnification. The dark brown spots indicated with the green arrows represent the distribution pattern and levels of the MPG proteins in oral cancer cells stained with a monoclonal antibody. The blue area indicates the location of the cell nuclei stained with haematoxylin. The mean integrated MPG protein intensities are shown in the bottom panel. ^{a,b,c}Values with unlike letters are significantly different ($P < 0.05$). Values are means, with standard errors represented by vertical bars.

and reprobated with a β -actin antibody as the loading control. The levels of phosphorylated mTOR, phosphorylated I κ B α , phosphorylated ERK 1/2 and total E-cadherin proteins in tumour tissues were measured with the same procedure as described previously. The levels of p16^{Ink4a}, cyclin D1 and NF- κ B p65 (RelA) in the nuclear fractions of tumour tissues were measured using a similar procedure as described previously. The blots were stripped and reprobated with a lamin A/C antibody as the loading control.

Detection of plasma osteopontin by ELISA

OPN plasma level was measured by ELISA (R&D Systems, Inc.), according to the manufacturer's instructions. Briefly, a 100 μ l diluted plasma sample (1:100 dilution) from each group (tumour-free mice, tumour control mice, low_SAC mice and high_SAC mice) was added to each well and analysed. Upon completion of the ELISA process, the plate was read at 450/570 nm wavelength using a microplate reader (Tecan Inc., Mannedorf, Switzerland).

Statistical analysis

Quantitative analysis was used to determine whether there were differences in tumour weight or volume among the low_SAC, high_SAC and tumour control groups (n 6 per group) in human oral cancer-bearing mice. Statistical analyses of the differences in tumour weight or volume among the experimental and control conditions were performed using SYSTAT software (SYSTAT Software Inc., Chicago, IL, USA). Confirmation of a difference in tumour weight or volume as statistically significant required a rejection of the null hypothesis of no difference between the mean weight or volume obtained from the different sets of experimental and control groups at the $P=0.05$ level using one-way ANOVA. The Bonferroni *post hoc* test was used to determine differences between the groups.

Results

S-allylcysteine inhibited tumour growth and the progression of oral cancer in a mouse xenograft model

Our previous study has demonstrated that SAC inhibited the proliferation of human oral cancer CAL-27 cells *in vitro*. We therefore extended our investigation to an *in vivo* xenograft tumour model to validate the significance of the *in vitro* findings. The inhibitory effects of SAC on the growth of oral cancer cells in a mouse xenograft tumour model were investigated. A mouse xenograft tumour model was established by subcutaneously inoculating human oral cancer CAL-27 cells into the right flank of each nude mouse. The results showed that SAC consumption significantly suppressed the growth of oral cancer in tumour-bearing mice ($P<0.05$). By the end of the study (4th week), the tumour volume per mouse had decreased from 177 (SE 18) mm³ in the tumour control group to 126 (SE 25) and 47 (SE 6) mm³ in the 5 mg SAC/kg BW (low_SAC) and 40 mg SAC/kg BW (high_SAC)-fed groups,

respectively, accounting for a 30 and 74% inhibition in tumour growth ($P<0.05$) (Fig. 1(A)). The tumour weight results at the end of the study further supported these findings. Compared with the tumour control group, which had a tumour weight of 0.28 (SE 0.02) g/mouse, the low_SAC- and high_SAC-fed mice had 0.2 (SE 0.01) and 0.08 (SE 0.02) g/mouse tumour weight, accounting for a 27 and 70% decrease, respectively ($P<0.05$) (Fig. 1(B)). Both the low_SAC and high_SAC doses significantly inhibited oral cancer tumour growth in this mouse xenograft model ($P<0.05$).

Furthermore, SAC significantly inhibited the protein levels of PCNA in tumour-bearing mice ($P<0.05$; Fig. 1(C)). The haematoxylin–eosin staining results also demonstrated that SAC inhibited tumour progression in this mouse xenograft model (Fig. 1(D)). Immunohistochemical staining showed that SAC suppressed the nuclear levels of MPG in tumour tissues (b, c *v.* a and e, f *v.* d; Fig. 1(E)). Compared with the tumour control group, SAC at both the low and high doses suppressed tumour tissue MPG levels by up to 34 and 71%, respectively. These results demonstrated that SAC significantly suppressed both tumour growth and progression ($P<0.05$), providing evidence for the chemopreventive effects of SAC. The mechanism of action appears to be associated with the suppression of nuclear PCNA and MPG.

S-allylcysteine decreased the osteopontin plasma level in tumour-bearing mice

To further investigate the chemopreventive effects of SAC on tumour progression in oral cancer, we measured the OPN plasma level using ELISA analysis. As shown in Fig. 2, mice inoculated with oral cancer CAL-27 cells had high plasma levels of OPN. However, SAC at either a low dose (5 mg/kg BW) or a high dose (40 mg/kg BW) significantly decreased the plasma OPN protein level ($P<0.05$). By the end of the

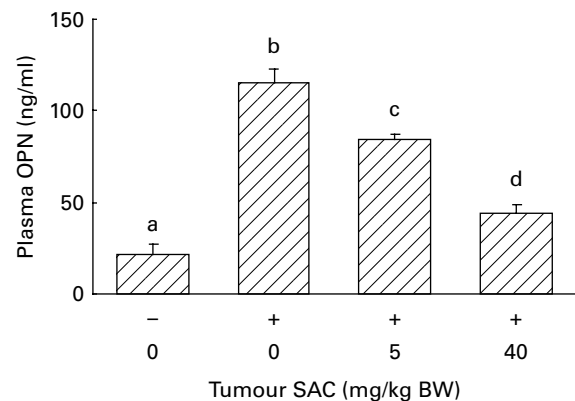


Fig. 2. *S*-allylcysteine (SAC) decreased the osteopontin (OPN) plasma level in tumour-bearing mice. The plasma levels of OPN were quantified with an ELISA Kit (R&D Systems, Inc., Minneapolis, MN, USA). Briefly, an equal amount of a diluted plasma sample (100 μ l) from each group (tumour-free mice, tumour control mice, low_SAC mice and high_SAC mice) was added to each well and reacted with the primary antibody against OPN according to the manufacturer's instructions. Upon completion of the ELISA process, fluorescence intensities were read using a wavelength of 450/570 nm. These results are representative of six different experiments. Values are means, with their standard errors represented by vertical bars. ^{a,b,c,d} Values with unlike letters are significantly different ($P<0.05$).

study, the basal OPN plasma levels in tumour-free mice were approximately 21 (SE 5)ng/ml. The OPN plasma levels decreased from 115 (SE 8)ng/ml in the tumour control group to 84 (SE 3) and 43 (SE 5)ng/ml in the low_SAC and high_SAC-fed groups, respectively. These results suggested that the chemopreventive effects of SAC are associated with decreases in the OPN plasma level in tumour-bearing mice.

S-allylcysteine inhibited the phosphatidylinositol-3-kinase/Akt and mitogen-activated protein kinase/extracellular signal-regulated kinase signalling pathways in tumour-bearing mice

To further validate the importance of SAC, we analysed the inhibitory effects of SAC on different elements of the

PI3K/Akt/mTOR and MAPK/ERK signalling pathways. As shown in Fig. 3(A), increases in the phosphorylation levels of Akt and mTOR proteins were widely observed in tumour tissues. Moreover, SAC at either of the two different doses (5 and 40 mg/kg BW) significantly decreased the phosphorylation levels of Akt and mTOR proteins in a dose-dependent manner (Fig. 3(B)). SAC also significantly suppressed the phosphorylation level of the IκBα protein in tumour tissues (Fig. 3(A)). These quantitative results suggested that the consumption of SAC was able to inhibit the activation of the Akt/mTOR signalling pathways and NF-κB in this mouse xenograft tumour model (Fig. 3(B)).

Our previous *in vitro* study has indicated that SAC inhibited the EMT process⁽⁴²⁾. In the present study, we further investigated whether SAC consumption would suppress

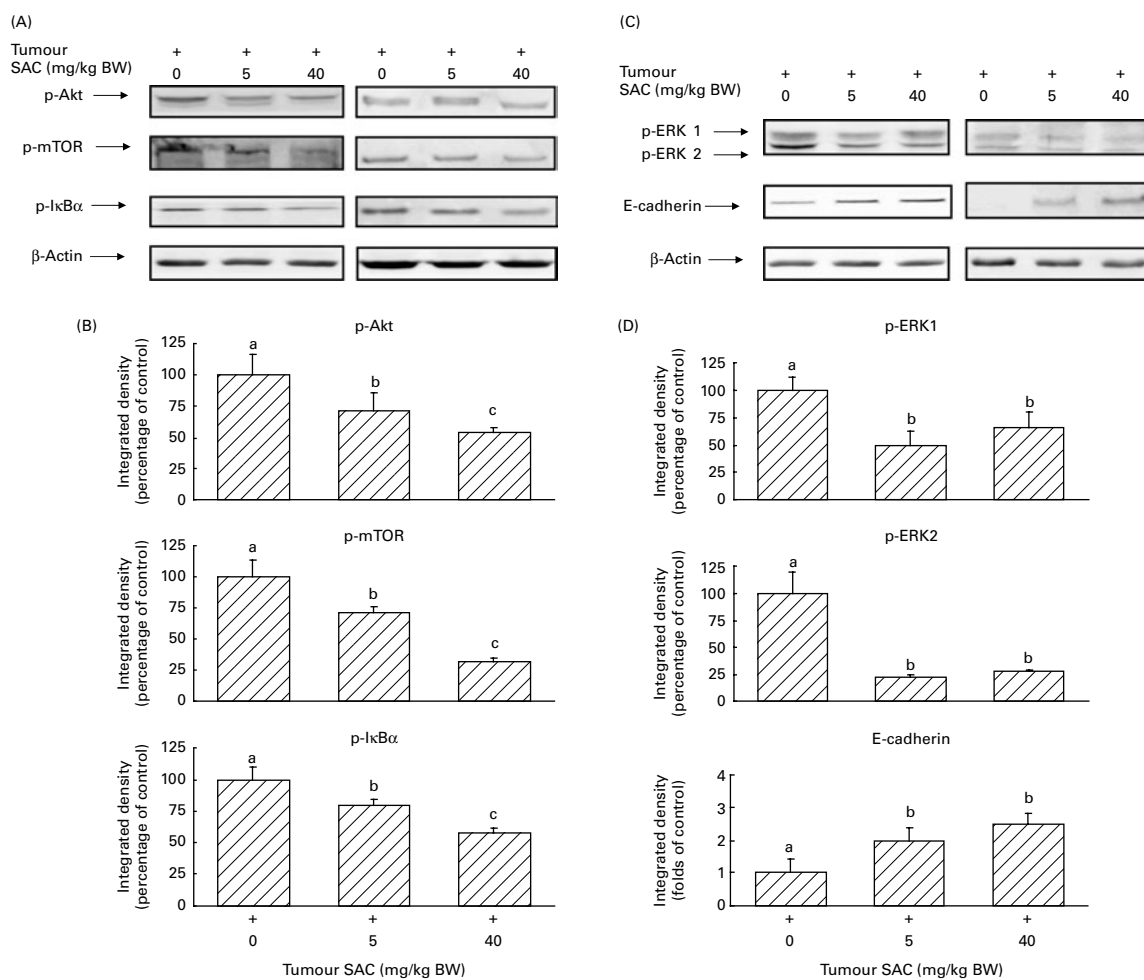


Fig. 3. S-allylcysteine (SAC) inhibited the phosphatidylinositol-3-kinase/Akt and mitogen-activated protein kinase/extracellular signal-regulated kinase (ERK) signalling pathways in tumour-bearing mice. (A) The preparation of the cell lysates from animal tissues was briefly described in the Materials and methods section. Cell lysates were blotted with anti-phosphorylation Akt (p-Akt), anti-phosphorylation mammalian target of rapamycin (p-mTOR) and anti-phosphorylation inhibitor of κBα (p-IκBα) monoclonal antibodies. The levels of detection in the cell lysates represent the amount of phosphorylated Akt, mTOR and IκBα proteins in tumour tissues. The blots were stripped and reprobed with an anti-β-actin antibody as the loading control. The results are representative of six different experiments. The immunoreactive bands are noted with the arrow. (B) Integrated densities of p-Akt, p-mTOR and p-IκBα proteins adjusted with the internal control protein (β-actin). ^{a,b,c} Values with unlike letters are significantly different ($P < 0.05$). (C) Cell lysates were blotted with anti-phosphorylation ERK (p-ERK) 1/2 and anti-E-cadherin monoclonal antibodies, as described in the Materials and methods section. The detection levels in the cell lysate represent the amount of phosphorylated ERK 1/2 proteins and total E-cadherin proteins in human oral cancer cells. The blots were stripped and reprobed with an anti-β-actin antibody as the loading control. The results are representative of six different experiments. The immunoreactive bands are noted with the arrow. (D) Integrated densities of p-ERK 1/2 proteins and total E-cadherin proteins adjusted with the internal control protein (β-actin). ^{a,b} Values with unlike letters are significantly different ($P < 0.05$). Values are means, with their standard errors represented by vertical bars.

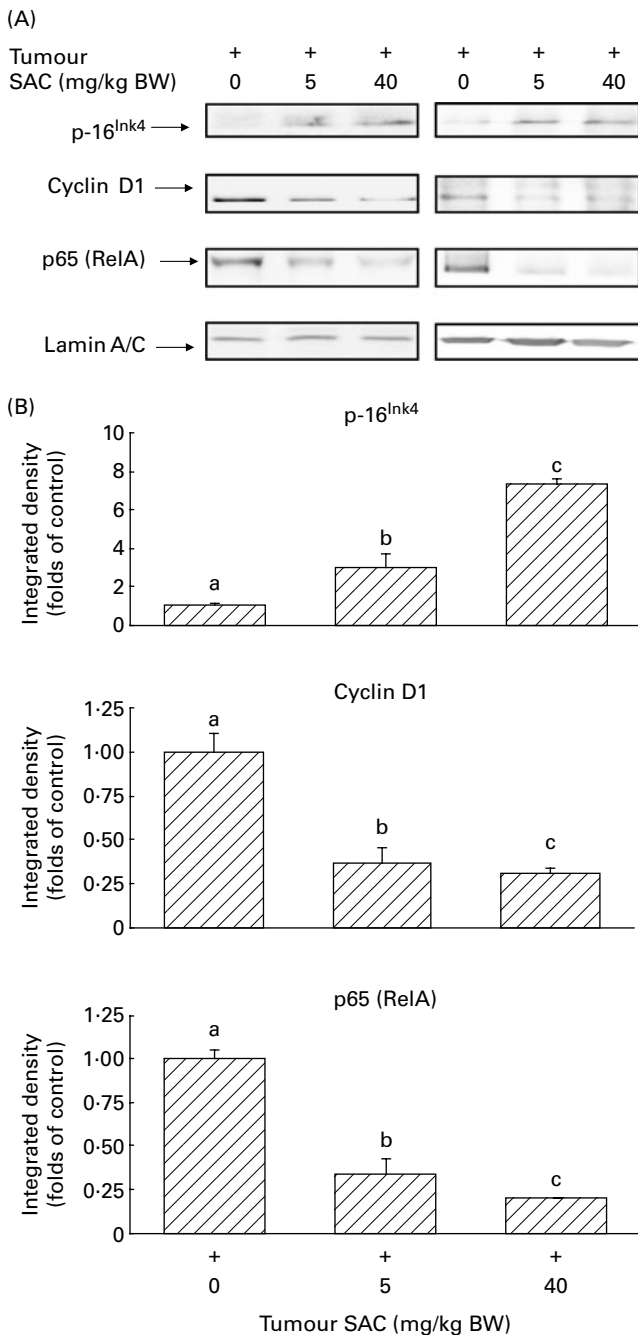


Fig. 4. S-allylcysteine (SAC) significantly suppressed the expression of cyclin D1 and NF- κ B in the mouse xenograft tumour model. (A) Preparation of the nuclear fraction cell lysates from animal tissues was briefly described in the Materials and methods section. Nuclear lysates were blotted with anti-p16^{Ink4}, anti-cyclin D1 and anti-NF- κ B p65 (RelA) monoclonal antibodies, as described in the Materials and methods section. The levels of detection in the cell lysate represented the amount of p16^{Ink4}, cyclin D1 and NF- κ B p65 (RelA) in tumour tissues. The blots were stripped and re-probed with an anti-lamin A/C antibody as the loading control. The results presented are representative of six different experiments. The immunoreactive bands are noted with the arrow. (B) Integrated densities of p16^{Ink4}, cyclin D1 and NF- κ B p65 (RelA) in tumour tissues. The blots were stripped and re-probed with an anti-lamin A/C antibody as the loading control. Values are means, with their standard errors represented by vertical bars. ^{a,b,c} Values with unlike letters are significantly different ($P < 0.05$).

MAPK/ERK signalling pathway activation in a mouse xenograft model. As shown in Fig. 3(C), SAC (at a dose of 5 or 40 mg/kg BW) significantly inhibited the phosphorylation levels of ERK1/2 proteins in tumour-bearing mice. Moreover, SAC induced the expression of E-cadherin proteins in tumour tissues. These results show that the inhibitory effects of SAC on tumour growth and progression, including the EMT, are associated with a suppression of the MAPK/ERK signalling pathway in tumour-bearing mice (Fig. 3(D)). Together, these observations strongly suggest that SAC impairs the PI3K/Akt/mTOR and MAPK/ERK pathways as broad effects in oral cancer CAL-27 cells in a mouse xenograft model.

S-allylcysteine significantly suppressed the expression of cyclin D1 and NF- κ B in the mouse xenograft tumour model

Previous investigations have indicated that cyclin D1 protein plays an important role in the regulation of cell proliferation. Moreover, the NF- κ B-mediated expression of COX-2 is strongly correlated with tumour progression. Therefore, we investigated whether SAC would suppress the expression of cyclin D1 proteins *in vivo*. As shown in Fig. 4(A), SAC significantly induced the expression of the cell-cycle inhibitor p16^{Ink4}, and suppressed the nuclear levels of cyclin D1 and NF- κ B p65 (RelA) proteins in tumour-bearing mice. The quantitative results demonstrated that SAC (at 5 and 40 mg/kg BW) even suppressed the expression of NF- κ B by up to 60 and 80%, respectively (Fig. 4(B)). These results suggest that the inhibitory effects of SAC on tumour growth and the progression of oral cancer were associated with the suppression of cyclin D1 and NF- κ B p65 (RelA). Therefore, SAC has potential as a chemopreventive agent for tumour growth and the progression of oral cancer, as demonstrated here in this mouse xenograft tumour model.

Immunofluorescent staining indicated that S-allylcysteine significantly blocked the epithelial–mesenchymal transition step and inflammation in oral cancer in these tumour-bearing mice

Due to the important roles of the MAPK/ERK and PI3K/Akt/NF- κ B signalling pathways in tumour progression and the EMT, we examined the inhibitory effects of SAC on the expression of biomarkers such as vimentin and COX-2 in a mouse xenograft tumour model. The immunofluorescent staining results showed that SAC significantly inhibited vimentin expression in tumour-bearing mice (Fig. 5(A)). SAC also significantly suppressed the expression of COX-2 at doses of 5 and 40 mg/kg BW, respectively (Fig. 5(A)). The co-localisation of vimentin and COX-2 indicated both the induction of the EMT and inflammation in tumour tissues. These results show that SAC minimised the inflammatory response and prevented EMT progression in tumour-bearing mice (Fig. 5(B)).

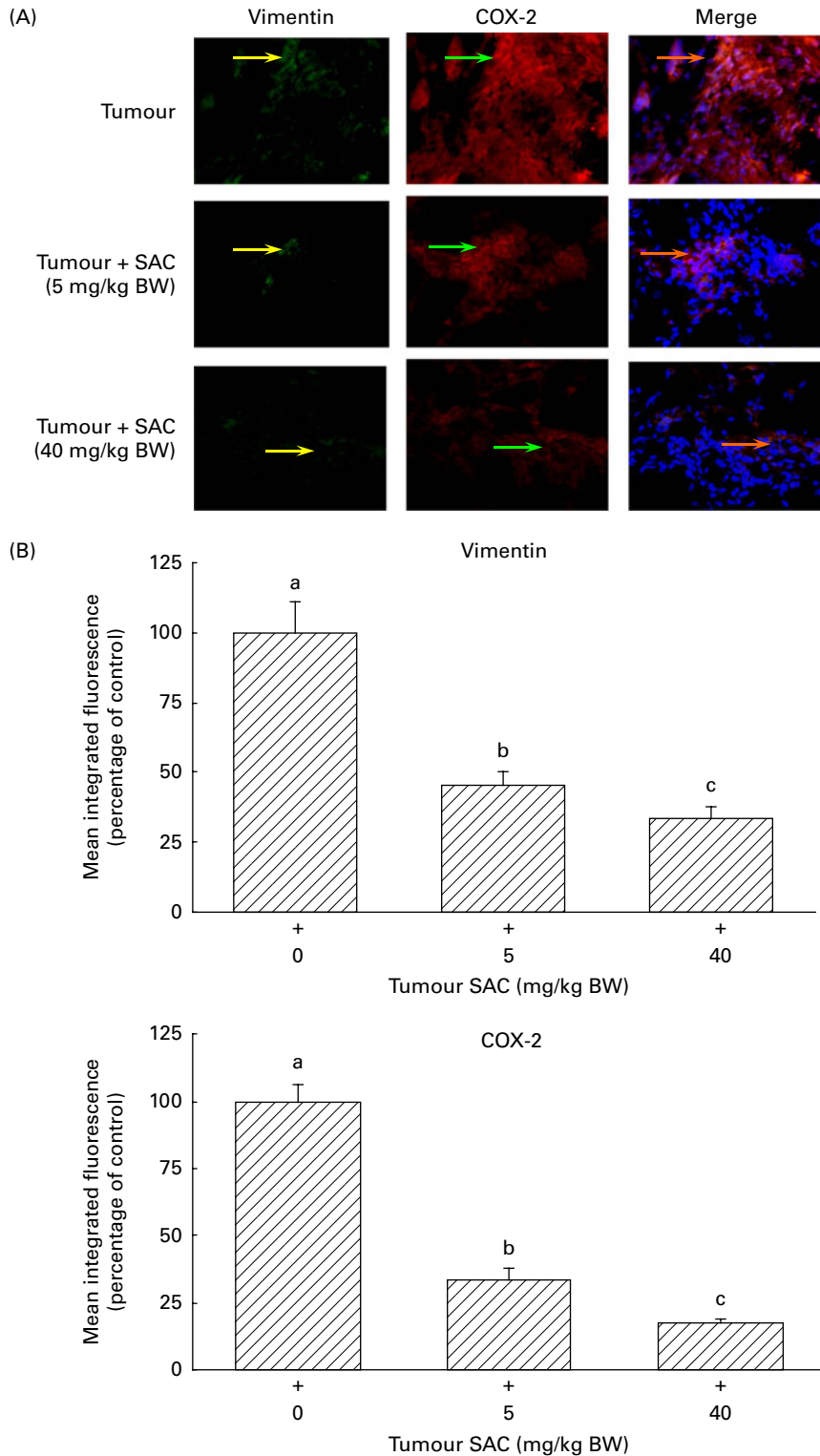


Fig. 5. Immunofluorescent staining indicated that S-allylcysteine (SAC) significantly blocked the epithelial–mesenchymal transition step and inflammation in oral cancer in these tumour-bearing mice. (A) Tumour tissues were frozen, sectioned and subjected to anti-vimentin and anti-cyclo-oxygenase-2 (COX-2) antibodies by immunofluorescent staining, as described in the Materials and methods section. Imaging was performed at 400 × magnification. The green fluorescence area indicated with the yellow arrows represents the distribution of vimentin protein in CAL-27 cells stained with the monoclonal antibody. The red fluorescence area indicated with the green arrows represents COX-2 protein in CAL-27 cells stained with the monoclonal antibody. The yellow fluorescence area indicated with the orange arrows in the merged imaging represents the co-localisation of vimentin and COX-2 proteins in tumour tissues. The blue fluorescence area represents the location of the cell nuclei stained with 4,6-diamidino-2-phenyl indole. These results are representative of six different experiments. (B) Mean integrated fluorescence of vimentin and COX-2. Values are means, with their standard errors represented by vertical bars. ^{a,b,c} Values with unlike letters are significantly different ($P < 0.05$).

Discussion

Many studies have suggested that the phytochemicals in fruits and vegetables might exert anticancer effects. The consumption of garlic has been associated with a reduced risk in the occurrence of cancer at different sites, including the liver, breast and colon^(41,43,44). A previous study has indicated that administration of SAC increased the levels of both reduced glutathione and glutathione-dependent enzymes⁽⁴⁴⁾. Our previous investigation has demonstrated that SAC inhibited the cell proliferation and EMT of human oral cancer cells *in vitro*⁽⁴²⁾. We also demonstrated that SAC consumption inhibited the tumour growth of human non-small-cell lung carcinoma independent of its antioxidant activities⁽⁴⁵⁾. SAC, a water-soluble garlic constituent, is characterised by its high bioavailability and is found in high concentrations in AGE^(46,47). AGE contains much higher levels of antioxidants than raw or cooked garlic. The present study was performed to determine whether SAC would suppress the tumour progression and EMT process.

As shown in Fig. 1, the results show that SAC at 5 mg/kg BW (low dosage) and 40 mg/kg BW (high dosage) dose-dependently inhibited the growth of oral cancer in tumour-bearing mice without any apparent untoward toxicity (data not shown). SAC is therefore safe at the studied doses. There was no difference in food intake or BW in the present study between the animal groups. A previous study has shown that there were no toxic symptoms at SAC doses between 250 and 2000 mg/kg BW. The haematoxylin–eosin staining results suggested that SAC blocks oral cancer tumour progression in tumour-bearing mice. Previous studies have demonstrated that PCNA is a trimeric complex with an essential role in DNA replication. PCNA makes up the platform required for the activity of DNA polymerases δ and ϵ during DNA replication. The present study shows that SAC also inhibits the expression of PCNA in tumour tissues. Immunofluorescent staining indicates that SAC is able to effectively block the proliferation of human oral cancer cells in nude mice. The results suggest that SAC inhibits tumour growth through a suppression of DNA replication.

MPG, a carcinogenesis promoter, has been shown to be up-regulated in several cancer cell lines⁽²⁹⁾. Overexpression of this enzyme has been found to contribute to the formation of chromatid exchanges, chromosomal aberration and gene mutations⁽³⁰⁾. In considering the role of MPG in carcinogenesis, we also investigated the expression of MPG protein in tumour tissues. Interestingly, the present results demonstrated that MPG proteins were highly expressed in the nuclei of tumour tissues in the tumour control group. However, consumption of SAC at both of the low and high doses prevented the nuclear translocalisation of MPG proteins. Most of the MPG proteins were diminished in the nuclei and retained in the cytoplasm of tumour tissues in both the low_SAC and high_SAC-fed groups (Fig. 1(E)).

These results comprise novel evidence of chemopreventive effects and demonstrate that SAC is able to suppress the nuclear levels of MPG proteins in tumour tissues. Investigation into the effects of SAC on the formation of chromatid

exchanges and chromosomal aberration will be undertaken in the near future. Previous study has indicated that an over-expression of OPN is associated with certain activities related to tumour growth and progression, including angiogenesis, invasion and metastasis in oral cancer. The expression of OPN (a prognostic biomarker of human oral cancer) is consistently associated with transformed epithelium in pre-malignant lesions and invasive squamous cell carcinoma. Secretion of OPN into the local tumour microenvironment may promote tumour cell proliferation, migration and angiogenesis by binding cell-surface receptors such as the $\alpha\beta3$ integrin proteins. The results here show that SAC suppressed the expression and secretion of OPN in this mouse xenograft tumour model (Fig. 2). This indicates that the inhibitory effects of SAC on the tumour progression of oral cancer were significantly associated with the suppression of OPN expression and decreases in nuclear MPG proteins in this mouse xenograft tumour model. There is thus a potentially beneficial role of SAC in the chemoprevention of oral cancer.

Many studies have demonstrated that the PI3K/Akt/mTOR signalling pathway plays an important role in the regulation of tumour growth and the progression of oral cancer⁽⁶⁾. The activated Akt/mTOR signalling pathway has been observed in oral cancer cells and an essential role suggested in the control of gene expression and protein translation, which exerts an impact on cell proliferation and inflammation during tumour development. Previous studies have indicated that there was a PI3K-dependent phosphorylation of Akt or NF- κ B molecules from among a panel of oral cancer cell lines, which effect was correlated with resistance to therapy⁽¹³⁾. The mTOR inhibitor rapamycin was shown to prevent tumorigenesis and to render oral cancer cell lines with highly activated Akt/mTOR more responsive to growth inhibition⁽⁴⁸⁾. Collectively, the evidence shows a significant role of the activated PI3K/Akt/mTOR pathway in oral cancer. In the present study, SAC effectively inhibited the phosphorylation of Akt, mTOR and I κ B α proteins (Fig. 3(A)). SAC, even at a low dosage (5 mg/kg BW), thereby inhibited the activation of the ERK 1/2 signalling pathway in tumour tissues (Fig. 3(C)). Moreover, SAC consumption induced the expression of E-cadherin proteins in tumour tissues. To examine whether SAC suppressed tumour growth and progression in oral cancer, we investigated the effects of SAC on the expression of cyclin D1 and NF- κ B. The present results demonstrated that SAC significantly suppressed the expression of cyclin D1 and NF- κ B proteins in tumour tissues. Furthermore, we investigated the effects of SAC on the expression of the cell-cycle inhibitor p16^{Ink4}. The consumption of SAC induced the expression of p16^{Ink4} (Fig. 4), which was correlated with the finding that SAC inhibited tumour growth and progression in tumour-bearing mice.

During the course of tumour progression, oral carcinoma cells typically lose their cell–cell adhesion capacity and become detached from neighbouring cells. The poor prognosis of oral cancer is frequently associated with this detachment along with inflammation and the EMT. The inflammatory response is characterised by increased COX-2 activity and PG expression. EMT progression features the



loss of E-cadherin and the overexpression of vimentin. We have previously demonstrated that SAC consumption helped augment the expression of E-cadherin proteins⁽⁴²⁾. To further investigate the effects of SAC on tumour progression and the EMT in oral cancer, we further identified the effects of SAC on the expression of COX-2 and vimentin. To investigate the correlation between inflammation and EMT progression in the mouse xenograft model, we determined the expression of these biomarkers using immunofluorescent staining. As shown in Fig. 5, SAC effectively suppressed the expression of vimentin and COX-2 in tumour-bearing mice. The results also demonstrated a coordination between inflammation and the EMT biomarkers. These results suggest a strong correlation between inflammation and the EMT occurring in oral carcinoma that developed in this mouse xenograft model. Consumption of SAC inhibited inflammation and tumour progression, including the EMT. The results from the present study are consistent with our previously reported findings⁽⁴²⁾.

In the present study, SAC consumption (at concentrations of 5 and 40 mg/kg BW per d) inhibited the activation of the PI3K/Akt/mTOR and MAPK/ERK signalling pathways and suppressed the expression of cyclin D1 and NF- κ B p65 (RelA) proteins. Furthermore, SAC inhibited the expression of vimentin and COX-2 proteins in tumour-bearing mice. In conclusion, SAC significantly suppressed oral cancer tumour growth and progression, including the EMT step, in this mouse xenograft tumour model of oral cancer. To the best of our knowledge, no *in vivo* experimental evidence has been previously reported regarding the SAC-mediated suppression of tumour growth and progression, including the EMT. This is the first *in vivo* evidence for the chemopreventive effects of SAC.

Acknowledgements

This study was supported, in part, by a National Science Council grant (no. NSC-97-2320-B-039-043-MY3), Department of Health grants (no. DOH 100-TD-B-111-004 and DOH-100-TD-C-111-005) and China Medical University (Taichung, Taiwan) grants (no. CMU98-P-08 and CMU98-P-08-M). Any opinions, findings, conclusions or recommendations expressed in this publication are those of the author(s) and do not necessarily reflect the view of the National Science Council, the Department of Health and the China Medical University. M.-H. P. conducted part of the research. Y.-H. K. provided assistance for analytical chemistry. E.-P. I. C. performed the data analysis. F.-Y. T. designed the experiment, conducted part of the research, analysed the data and prepared the manuscript. The authors declare that they have no conflicts of interest.

References

1. Kademani D (2007) Oral cancer. *Mayo Clin Proc* **82**, 878–887.
2. Devoll RE, Li W, Woods KV, *et al.* (1999) Osteopontin (OPN) distribution in premalignant and malignant lesions of oral epithelium and expression in cell lines derived from

- squamous cell carcinoma of the oral cavity. *J Oral Pathol Med* **28**, 97–101.
3. Rittling SR & Chambers AF (2004) Role of osteopontin in tumour progression. *Br J Cancer* **90**, 1877–1881.
4. Wai PY & Kuo PC (2008) Osteopontin: regulation in tumor metastasis. *Cancer Metastasis Rev* **27**, 103–118.
5. Das R, Mahabeleshwar GH & Kundu GC (2003) Osteopontin stimulates cell motility and nuclear factor kappaB-mediated secretion of urokinase type plasminogen activator through phosphatidylinositol 3-kinase/Akt signaling pathways in breast cancer cells. *J Biol Chem* **278**, 28593–28606.
6. Fresno Vara JA, Casado E, de Castro J, *et al.* (2004) PI3K/Akt signalling pathway and cancer. *Cancer Treat Rev* **30**, 193–204.
7. Robertson BW, Bonsal L & Chelliah MA (2010) Regulation of Erk1/2 activation by osteopontin in PC3 human prostate cancer cells. *Mol Cancer* **9**, 260.
8. Nicholson KM & Anderson NG (2002) The protein kinase B/Akt signalling pathway in human malignancy. *Cell Signal* **14**, 381–395.
9. Vivanco I & Sawyers CL (2002) The phosphatidylinositol 3-Kinase AKT pathway in human cancer. *Nat Rev Cancer* **2**, 489–501.
10. Bai D, Ueno L & Vogt PK (2009) Akt-mediated regulation of NFkappaB and the essentialness of NFkappaB for the oncogenicity of PI3K and Akt. *Int J Cancer* **125**, 2863–2870.
11. Sawhney M, Rohatgi N, Kaur J, *et al.* (2007) Expression of NF-kappaB parallels COX-2 expression in oral precancer and cancer: association with smokeless tobacco. *Int J Cancer* **120**, 2545–2556.
12. Brown JR & DuBois RN (2004) Cyclooxygenase as a target in lung cancer. *Clin Cancer Res* **10**, 4266s–4269s.
13. Tamatani T, Azuma M, Motegi K, *et al.* (2007) Cepharranthin-enhanced radiosensitivity through the inhibition of radiation-induced nuclear factor-kappaB activity in human oral squamous cell carcinoma cells. *Int J Oncol* **31**, 761–768.
14. McCubrey JA, Steelman LS, Chappell WH, *et al.* (2007) Roles of the Raf/MEK/ERK pathway in cell growth, malignant transformation and drug resistance. *Biochim Biophys Acta* **1773**, 1263–1284.
15. Jayasurya R, Francis G, Kannan S, *et al.* (2004) p53, p16 and cyclin D1: molecular determinants of radiotherapy treatment response in oral carcinoma. *Int J Cancer* **109**, 710–716.
16. Todd R, Hinds PW, Munger K, *et al.* (2002) Cell cycle dysregulation in oral cancer. *Crit Rev Oral Biol Med* **13**, 51–61.
17. Sartor M, Steingrimsdottir H, Elamin F, *et al.* (1999) Role of p16/MTS1, cyclin D1 and RB in primary oral cancer and oral cancer cell lines. *Br J Cancer* **80**, 79–86.
18. Dohadwala M, Wang G, Heinrich E, *et al.* (2010) The role of ZEB1 in the inflammation-induced promotion of EMT in HNSCC. *Otolaryngol Head Neck Surg* **142**, 753–759.
19. Jang TJ, Jeon KH & Jung KH (2009) Cyclooxygenase-2 expression is related to the epithelial-to-mesenchymal transition in human colon cancers. *Yonsei Med J* **50**, 818–824.
20. Chang JY, Wright JM & Svoboda KK (2007) Signal transduction pathways involved in epithelial-mesenchymal transition in oral cancer compared with other cancers. *Cells Tissues Organs* **185**, 40–47.
21. Hong KO, Kim JH, Hong JS, *et al.* (2009) Inhibition of Akt activity induces the mesenchymal-to-epithelial reverting transition with restoring E-cadherin expression in KB and KOSCC-25B oral squamous cell carcinoma cells. *J Exp Clin Cancer Res* **28**, 28.
22. Thomas GJ & Speight PM (2001) Cell adhesion molecules and oral cancer. *Crit Rev Oral Biol Med* **12**, 479–498.
23. Neal CL, McKeithen D & Odero-Marrah VA (2011) Snail negatively regulates cell adhesion to extracellular matrix and

- integrin expression via the MAPK pathway in prostate cancer cells. *Cell Adh Migr* **5**, 249–257.
24. Conacci-Sorrell M, Simcha I, Ben Yedidia T, *et al.* (2003) Autoregulation of E-cadherin expression by cadherin-cadherin interactions: the roles of beta-catenin signaling, Slug, and MAPK. *J Cell Biol* **163**, 847–857.
 25. Matsuzaki H, Shima K, Muramatsu T, *et al.* (2007) Osteopontin as biomarker in early invasion by squamous cell carcinoma in tongue. *J Oral Pathol Med* **36**, 30–34.
 26. Muramatsu T, Shima K, Ohta K, *et al.* (2005) Inhibition of osteopontin expression and function in oral cancer cell lines by antisense oligonucleotides. *Cancer Lett* **217**, 87–95.
 27. Sharma C, Kaur J, Shishodia S, *et al.* (2006) Curcumin down regulates smokeless tobacco-induced NF-kappaB activation and COX-2 expression in human oral premalignant and cancer cells. *Toxicology* **228**, 1–15.
 28. Nystrom ML, McCulloch D, Weinreb PH, *et al.* (2006) Cyclooxygenase-2 inhibition suppresses alphavbeta6 integrin-dependent oral squamous carcinoma invasion. *Cancer Res* **66**, 10833–10842.
 29. Cerda SR, Turk PW, Thor AD, *et al.* (1998) Altered expression of the DNA repair protein. *N*-methylpurine-DNA glycosylase (MPG) in breast cancer. *FEBS Lett* **431**, 12–18.
 30. Bessho T, Roy R, Yamamoto K, *et al.* (1993) Repair of 8-hydroxyguanine in DNA by mammalian *N*-methylpurine-DNA glycosylase. *Proc Natl Acad Sci U S A* **90**, 8901–8904.
 31. Fleischauer AT & Arab L (2001) Garlic and cancer: a critical review of the epidemiologic literature. *J Nutr* **131**, 1032S–1040S.
 32. Hsing AW, Chokkalingam AP, Gao YT, *et al.* (2002) Allium vegetables and risk of prostate cancer: a population-based study. *J Natl Cancer Inst* **94**, 1648–1651.
 33. Thomson M & Ali M (2003) Garlic [*Allium sativum*]: a review of its potential use as an anti-cancer agent. *Curr Cancer Drug Targets* **3**, 67–81.
 34. Hosono T, Fukao T, Ogihara J, *et al.* (2005) Diallyl trisulfide suppresses the proliferation and induces apoptosis of human colon cancer cells through oxidative modification of beta-tubulin. *J Biol Chem* **280**, 41487–41493.
 35. Jo HJ, Song JD, Kim KM, *et al.* (2008) Diallyl disulfide induces reversible G2/M phase arrest on a p53-independent mechanism in human colon cancer HCT-116 cells. *Oncol Rep* **19**, 275–280.
 36. Xiao D, Lew KL, Kim YA, *et al.* (2006) Diallyl trisulfide suppresses growth of PC-3 human prostate cancer xenograft *in vivo* in association with Bax and Bak induction. *Clin Cancer Res* **12**, 6836–6843.
 37. Arunkumar A, Vijayababu MR, Srinivasan N, *et al.* (2006) Garlic compound, diallyl disulfide induces cell cycle arrest in prostate cancer cell line PC-3. *Mol Cell Biochem* **288**, 107–113.
 38. Yang JS, Kok LF, Lin YH, *et al.* (2006) Diallyl disulfide inhibits WEHI-3 leukemia cells *in vivo*. *Anticancer Res* **26**, 219–225.
 39. Tanaka S, Haruma K, Yoshihara M, *et al.* (2006) Aged garlic extract has potential suppressive effect on colorectal adenomas in humans. *J Nutr* **136**, 821S–826S.
 40. Chu Q, Lee DT, Tsao SW, *et al.* (2007) *S*-allylcysteine, a water-soluble garlic derivative, suppresses the growth of a human androgen-independent prostate cancer xenograft, CWR22R, under *in vivo* conditions. *BJU Int* **99**, 925–932.
 41. Gapter LA, Yuin OZ & Ng KY (2008) *S*-Allylcysteine reduces breast tumor cell adhesion and invasion. *Biochem Biophys Res Commun* **367**, 446–451.
 42. Tang FY, Chiang EP, Chung JG, *et al.* (2009) *S*-allylcysteine modulates the expression of E-cadherin and inhibits the malignant progression of human oral cancer. *J Nutr Biochem* **20**, 1013–1020.
 43. Katsuki T, Hirata K, Ishikawa H, *et al.* (2006) Aged garlic extract has chemopreventative effects on 1,2-dimethylhydrazine-induced colon tumors in rats. *J Nutr* **136**, 847S–851S.
 44. Sundaresan S & Subramanian P (2008) Prevention of *N*-nitrosodiethylamine-induced hepatocarcinogenesis by *S*-allylcysteine. *Mol Cell Biochem* **310**, 209–214.
 45. Tang FY, Chiang EP & Pai MH (2010) Consumption of *S*-allylcysteine inhibits the growth of human non-small-cell lung carcinoma in a mouse xenograft model. *J Agric Food Chem* **58**, 11156–11164.
 46. Nagae S, Ushijima M, Hatono S, *et al.* (1994) Pharmacokinetics of the garlic compound *S*-allylcysteine. *Planta Med* **60**, 214–217.
 47. Amagase H, Petesch BL, Matsuura H, *et al.* (2001) Intake of garlic and its bioactive components. *J Nutr* **131**, 955S–962S.
 48. Raimondi AR, Molinolo A & Gutkind JS (2009) Rapamycin prevents early onset of tumorigenesis in an oral-specific K-ras and p53 two-hit carcinogenesis model. *Cancer Res* **69**, 4159–4166.